H_∞ CONTROLLERS FOR THE REJECTION OF MICROVIBRATION DISTURBANCES

J. Stoustrup*, G. Aglietti†, E. Rogers†, R. S. Langley‡, S. B. Gabriel†

* *Department of Control Engineering, Aalborg University, Denmark*
Email jakob@control.auc.dk, Tel +45 9635 8749, Fax +45 9815 1739
† *Dept Electronics and Computer Science/Dept Aero/Astro,*
University of Southampton, U.K.
‡ *Dept Engineering, University of Cambridge, U.K.*

Abstract

The suppression of microvibrations (low amplitude vibrations with frequencies in the range 1 to 1000 Hz) is becoming increasingly important in spacecraft and other applications and can only be achieved (in most cases) by active feedback control schemes. This paper describes a Lagrange-Rayleigh-Ritz method which has been used to develop a state space description of the generic case of a vibrating panel with piezo-electric patches as actuators and sensors, disturbances, and a payload. The resulting models are used here to design H_∞ based active feedback control schemes for disturbance attenuation.

1 Introduction

Recent years have seen a dramatic increase in the stability requirements placed on payload instruments, with consequent increases in the level of vibration suppression demanded from the spacecraft structure. As a result, in this and other areas, low amplitude vibrations at frequencies between 1 Hz and 1000 Hz, generally termed microvibrations, once neglected due to the low levels of disturbances induced onbaord satellites, are now of critical importance. As such, they are the subject of much research effort aimed at developing efficient techniques for their control, eg [1]. In effect, such vibrations onboard spacecraft are produced by the functioning of onboard equipment such as reaction wheels, gyroscopes, thrusters, electric motors, and then propagate through the satellite structure towards sensitive equipment (receivers) thereby jeopardizing their correct functioning.

In practice, the reduction of the vibration level in a structure can be attempted by action at the source(s), receiver(s), and along the vibration path(s). At the source(s), this action consists of attempting to minimize the amplitude(s) of the vibration(s) by, for example, placing equipment on appropriate mountings. The same approach is commonly attempted at the receiver(s) but with the basic objective of sensitivity reduction. Finally, along the vibration path(s), modifications of structural elements or relocation of equipment is attempted with the aim of reducing the mechanical coupling between source(s) and receiver(s).

All of the approaches described above are most often implemented using passive damping technology and, for routine applications, an appropriate combination of them is often capable of producing the desired levels of dynamic disturbance rejection. The use of active control techniques in such cases would only be as a last resort to achieve desired performance. In the case of microvibrations, however, only active control can be expected to provide the required levels of suppression.

To investigate the use of active control to suppress microvibrations in a structure, computationally feasible models which retain the core features of the underlying dynamics are clearly required. The most obvious approach to the development of such models is to use finite element methods (FEM) (see, for example, [2]) due to the accuracy available with a sufficiently fine mesh. The only difficulty with this approach is the computational intensity of the processing required to generate the models and their use in predicting system response. They can, however, be used, as here, to verify that the modeling strategy employed produces 'realistic' models on which to base controller design and evaluation.

Alternatives to FEM, can be classified as elastic wave methods, variational methods, and mechanical impedance based methods respectively. A study of the advantages and disadvantages of these methods, together with background references on each of them, can be found in [3]. Based on this study, a Lagrange-Rayleigh-Ritz (LRR) method is used to develop the mathematical models used as a basis for the controller design studies reported in this paper.

Previous work [4] has developed this LRR method, to-

gether with supporting software, to the stage where state a state space model in the standard form for robust controller design is generated given the dimensions, material properties, and loading pattern of the structure to be considered. Also a systematic methodology for evaluating the quality of the model so produced is included.

This paper uses this facility as a basis for the design and evaluation of H_∞ controllers for a standard configuration of a panel with a payload, a single disturbance entering somewhere else on the panel, and two pairs of piezo-electric patches used respectively as actuator and sensors, again located at other positions. Although the exposition below only covers a single-variable design, both the modeling procedure and the control design technique applies equally well in the case of several payloads, several disturbances, several actuators and several sensors.

2   System Description and Modeling

The work reported here is based on a mass loaded panel - an acceptable compromise between problem complexity and the need to gain useful insights into the benefits (and limitations) of active control schemes in this general area. A schematic diagram of the arrangement considered is shown in Figure 1, where the equipment mounted on the panel is modeled as lumped masses and the disturbances as point forces. The controller design results given in section 3 of this paper are for a representative problem given in [4], and, in particular, a rectangular panel with a lumped mass mounted on it, two pairs of piezo-electric patches acting as the sensors and actuators of the control system, and a harmonic point force acting perpendicular to the panel as the disturbance source.
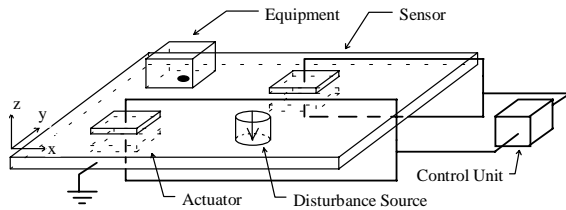
Figure 1: Model layout

The sensors and actuators employed are twin patches of piezoelectric material bounded onto opposite faces of the panel. The bending vibrations of the panel produce stretching and shrinking of the patches depending on whether they are on the top or the bottom of it. Due to the piezoelectric effect, these deformations induce an electric field perpendicular to the panel which is detected by the electrodes of the patches. The outer electrodes of the patches are electrically connected together and the

panel, which is grounded, is used as the other electrode for both patches of the pair. The same configuration is used for the actuator, but in this case the electric field is applied externally to produce contraction or expansion of the patch, which then induces a curvature of the panel.

A key point is that the effectiveness of the piezoelectric elements, both as actuators and sensors, is significantly reduced if the wavelength of the deformations is smaller than the patch. The essential reason for this reduced effectiveness is that the signal produced in this case is partially or completely canceled by the opposing field generated by the other part of the patch as it is deformed in the opposite direction. This limiting factor is especially important when attempting to control high frequency vibrations which have, of course, very short wavelengths. One possible means of increasing the effectiveness of the patches in these situations would be to decrease the patch dimension, but care is needed since this would also diminish the control action at low frequencies.

The LRR based procedure used to model this system (Figure 1) is based on Lagrange's equations of motion which in the general case take the form

$$\frac{d}{dt}\left(\frac{\partial T}{\partial \dot{q}_i}\right) - \frac{\partial T}{\partial q_i} + \frac{\partial U}{\partial q_i} = Q_i \qquad (1)$$

Here T and U are the kinetic and potential energies of the system, and q_i and Q_i are the ith generalized co-ordinate and force respectively. For the particular case considered here, the kinetic and potential energies (elastic and electric) can be expressed as

$$
\begin{aligned}
T &= T_{pl} + T_{lm} + T_{pz}\\
U &= U_{pl} + U_{pz_{elast}} + U_{pz_{elastelect}} + U_{pz_{elect}} \qquad (2)
\end{aligned}
$$

where T_{pl}, T_{lm} and T_{pz} denote the kinetic energies of the panel, lumped masses, and piezoelectric patches respectively, U_{pl} is the elastic energy stored in the panel, $U_{pz_{elast}}$ is the elastic energy stored in the piezoelectric patches, $U_{pz_{elastelect}}$ represents the potential energy due to the voltage driven piezoelectric effect, and $U_{pz_{elect}}$ is the electric energy stored due to the dielectric characteristics of the piezoelectric material.

The displacement field (out-of-plane displacement w) is obtained by a superposition of shape functions $S_{m,n}$ (consisting of the first $Nm \times Nn$ modes of the bare panel) multiplied by the time dependent modal co-ordinates $\phi_{m,n}$, i.e.

$$w(x,y,t) = \sum_{m=1}^{Nm}\sum_{n=1}^{Nn} S_{m,n}(x,y)\phi_{m,n}(t) = s^T\Phi \qquad (3)$$

where the $\hat{N} \times 1$ ($\hat{N} = Nm \times Nn$) column vectors s and Φ contain the shape functions and modal co-ordinates respectively.

The external excitation consists of Nf point forces F_j acting on the panel at arbitrary locations. Hence the gen-

eralized forces are of the form

$$Q_i = \sum_{j=0}^{Nf} F_j \frac{\partial w}{\partial \phi_i} \quad \text{or} \quad Q = S_f f \tag{4}$$

where f is the Nf $\times$ 1 column vector of forces and S_f is a compatibly dimensioned matrix whose columns are given by the model shape vector s evaluated at the corresponding force locations.

It is now necessary to compute each of the terms in (2), starting with the kinetic energies. Each of these terms can be calculated using standard formulas [2]. Their final forms in terms of the corresponding inertia matrices are given by

$$T_{pl} = \frac{1}{2}\dot{\Phi}^T M_{pl} \dot{\Phi}, \; T_{lm} = \frac{1}{2}\dot{\Phi}^T M_{lm} \dot{\Phi}, \; T_{pz} = \frac{1}{2}\dot{\Phi}^T M_{pz} \dot{\Phi} \tag{5}$$

The potential energy of the system is stored as the elastic energy of the panel and the elastic/electric energy of the piezoelectric patches. In the case of the panel, use of a standard formula [2] gives

$$U_{pl} = \frac{1}{2}\Phi^T K_{pl} \Phi \tag{6}$$

where K_{pl} is the panel stiffness matrix. Also, by assuming that each patch is perfectly bonded onto the panel and hence the stress-strain patterns in the latter can be extended to the volume of the patch , the same procedure as for the panel can be used to write

$$U_{pz_{elast}} = \frac{1}{2}\Phi^T K_{pz_{elast}} \Phi \tag{7}$$

where $K_{pz_{elast}}$ is the stiffness matrix which is fully populated and (see [2] for the details) given by

$$
\begin{aligned}
K_{pz_{elast}} &= \sum_{i=1}^{N_p} \int\int\int_{pz_i} \frac{E_{pz_i} z^2}{(1-\nu_i^2)} \Big(\frac{\partial^2 s}{\partial x^2} \frac{\partial^2 s^T}{\partial x^2} \\
&+ \frac{\partial^2 s}{\partial y^2} \frac{\partial^2 s^T}{\partial y^2} + 2\nu_i \frac{\partial^2 s}{\partial x^2} \frac{\partial^2 s^T}{\partial y^2} \\
&+ 2(1-\nu_i) \frac{\partial^2 s}{\partial x\partial y} \frac{\partial^2 s^T}{\partial x\partial y} \Big) dx\, dy\, dz
\end{aligned} \tag{8}
$$

In this last equation, N_p is the number of patches, pz_i denotes the volume of the ith patch, E_{pz_i} its Young's modulus, and ν_i its Poisson's ratio.

The additional stress which arises in the ith piezoelectric patch when an electric field $e_i(t) = v^T(t)p_i$ (where v is the column vector containing the Np patch voltages, and the column vector p_i has zero entries except for the inverse of the corresponding patch thickness in the ith position) is applied across the material can be expressed as

$$\sigma_{elect} = \left(\begin{array}{c} \sigma_{x_{elect}} \\ \sigma_{y_{elect}} \end{array}\right) = \frac{E_{pz}}{1-\nu^2} \left(\begin{array}{c} d_{xz} + \nu d_{yz} \\ d_{yz} + \nu d_{xz} \end{array}\right) e_i \tag{9}$$

Here d_{xz} and d_{yz} are the piezoelectric constants of the material, which is assumed to have pole direction z perpendicular to the panel. This additional stress, multiplied by the assumed strain, defines $U_{pz_{elastelect}}$ which can be calculated by substituting (9) into the expression

$$U_{pz_{elastelect}} = \int\int\int_{pz_i} \sigma^T \epsilon \, dx\, dy\, dz \tag{10}$$

By assuming $d_{xz} = d_{yz} = d_z$ it is possible to write the elastoelectric energy stored in the Np patches as

$$U_{pz_{elastelect}} = v^T K_{pz_{elastelect}} \Phi \tag{11}$$

where again the matrix $K_{pz_{elastelect}}$ can be computed using a standard formula [2]. Also the electrical energy stored in the piezoelectric material can be expressed as

$$U_{pz_{elect}} = \frac{1}{2}\int_{pz_i} e\, \hat{d}\, dx\, dy\, dz \tag{12}$$

where e is the electric field and $\hat{d}$ is the electric displacement (charge/area). For each patch, the electric displacement is

$$\hat{d}_i = \epsilon_{pz_i} p_i^T v \tag{13}$$

where ϵpz_i is the dielectric constant of the piezoelectric material which forms the ith patch. Hence an equivalent expression for the stored electric energy is

$$U_{pz_{elect}} = \frac{1}{2}v^T K_{pz_{elect}} v \tag{14}$$

where the elements of the matrix $K_{pz_{elect}}$ are the capacitances of the piezoelectric patches and can be computed using a standard formula (see [4] for the details).

At this stage, all of the energy terms are available as functions of the generalized co-ordinates ϕ and v and straightforward application of Lagrange's equations of motion (1) using the software developed in [4] now gives the following equations of motion

$$
\begin{aligned}
M_1 \ddot{\phi} + K_1 \phi + K_{pz_{elastelect}}^T v &= Q \\
K_{pz_{elastelect}} \phi + K_{pz_{elect}} v &= 0
\end{aligned} \tag{15}
$$

where

$$
\begin{aligned}
M_1 &= M_{pl} + M_{pz} + M_{lz} \\
K_1 &= K_{pl} + K_{pz_{elast}}
\end{aligned} \tag{16}
$$

The first equation in (15) is the result of differentiating the energy terms with respect to the modal co-ordinates ϕ and the second by differentiating these terms with respect to the voltages v, under the assumption that all modal co-ordinates and voltages are degrees of freedom of the system.

In the case when all the patches act as actuators, their voltages v_i will be externally driven and hence the second equation in (15) is redundant. Alternatively, if all the

patches act as sensors, the second equation in (15) can be used to obtain an expression for the voltages as a function of the modal co-ordinates which, in turn, can be substituted into the first equation in (15) to produce a complete set of equations for the unknowns ϕ.

The most general case occurs when some of the patches act as actuators and the others as sensors, and it is therefore necessary to partition the matrix $K_{pz_{elastect}}$ to separate actuator and sensor contributions. Suppose, therefore, that v_a and v_s denote the vectors of the voltages at the actuators and sensors respectively and $K_{pza_{elastelect}}$ and $K_{pzs_{elastelect}}$ the corresponding partitions of the matrix $K_{pz_{elastelect}}$. Then the first equation in (15) can be written in the form

$$
\begin{aligned}
M\ddot{\phi} \;\; + \;\; & C_s\dot{\phi} + (K_{elas} + K_{pzs})\phi \\
= \;\; & -(K_{pza_{elastelect}})^T v_a + s_f^T f
\end{aligned} \tag{17}
$$

where all the inertia terms are included in the matrix M and the stiffness due to elasticity in K_{elas}. Also

$$
K_{pzs} = -(K_{pzs_{elastelect}})^T (K_{pzs_{elect}})^{-1} K_{pzs_{elastelect}} \tag{18}
$$

represents the contribution to the stiffness from the piezoelectric energy stored in the patches acting as sensors, where $K_{pzs_{elect}}$ is the partition of $K_{pz_{elect}}$ corresponding to the sensors. Additionally, structural damping has been added to the system by the inclusion of the term defined by the damping matrix C_s. These last two equations can now be used to write the system dynamics in the standard form for robust controller design given the dimensions, material properties and the loading/disturbance force pattern.

In the remainder of this paper, H_∞ controllers are designed and evaluated for the rejection at a specific point on the panel of the effects of dynamic disturbances applied/arising at other locations on the panel. A treatment of the verification procedure prior to accepting a model developed by this approach for controller design studies is omitted here for brevity and full details, together with illustrative examples, can again be found in [4].

3 H_∞ Control Design

There are several reasons why H_∞ control design is the obvious candidate for the control problem under consideration, starting with the fact that the natural problem formulation is in the so-called 4-block form, see e.g. [5]. Since control signals and disturbances are physically located at different positions, they enter the dynamics in rather different ways. Similarly, the measured outputs are not the displacements at the positions of the payloads, and therefore inferred outputs must be introduced. Since the control system comprises two sets of inputs (disturbances and actuator signals) and two sets of outputs (payload displacements and sensor signals), a total four matrix-valued transfer functions must be taken into consideration. Failure to do so - as e.g. is typical for classical

control techniques - can be critical for the application under consideration. However, for H_∞ control techniques, 4-block formulations are absolutely standard.

Moreover, since the control objective is to suppress oscillations related to several modes, it is natural to employ a frequency domain design method in a loop-shaping approach, where again H_∞ control techniques are an obvious choice. Also a more detailed examination of the open-loop transfer functions from disturbances to payload displacement reveals the following characteristics:

- In the interesting frequency range, the transfer function is flat in average but with enormous resonance peaks at individual frequencies.

- Each resonance peak is narrow in terms of frequency range, but very tall.

- The system has a huge number of right half plane zeros.

- The interpolation constraints[1] associated with the most significant zeros are relatively moderate.

These observations indicate that a simple 'flattening out' as can be achieved by an unweighted H_∞ sensitivity design would be a viable approach to achieve the desired disturbance attenuation. Simply by reducing the overall unweighted H_∞ norm, each resonance peak could be substantially reduced, and that would mean that most disturbances would be effectively rejected, since the amplitudes of displacements are mainly governed by resonant phenomena.

The model derived from application LRR modeling procedure of the previous section is of the following form:

$$
\begin{aligned}
\dot{x} \;\; & = \;\; Ax \;\; + \;\; B_f f \;\; + \;\; B_v v \\
d \;\; & = \;\; C_d x \\
e \;\; & = \;\; C_e x
\end{aligned} \tag{19}
$$

In this model x is the state vector which takes values in $\mathcal{R}^N$ with $N = 2 \times Nm \times Nn$, f is a vector defined by the point force signals, and v is a vector containing the control voltages supplied to the actuator patches, d is the vector (if several payloads) of payload displacements, and finally e is the vector of voltages generated by the sensor patches.

The only real step needed to transform the derived model into a usual H_∞ 4-block problem is regularization, i.e. the input to H_∞ software, requires that the transfer matrix from control signal to inferred outputs has a direct feedthrough term of full column rank, and that - in a dual fashion - the transfer function from disturbances to measurements has a direct feedthrough term of full row rank.

---

[1] H_∞ interpolation constraints are fundamental system limitations which rely on poles and zeros in the right half plane. They give rise to frequency domain bounds which can be easily computed numerically.

It should be noted that this is *not* appropriately achieved as sometimes suggested in the literature simply by adding terms directly to the existing signals, e.g. by modifying $d = C_d x$ and $e = C_e x$ to $d = C_d x + \varepsilon_1 v$ and $e = C_e x + \varepsilon_2 f$, respectively. The problem with this approach is that values of the perturbations that are sufficiently large to satisfy the requirements set by the software would drastically change the zero structure of the plant, and hence give completely useless results.

One reasonable approach in the case considered here is to apply the so-called cheap control approach, where a number of fictitious disturbance signals, φ, and a number of fictitious payload displacements, δ, are introduced. As an alternative, the problem could be directly addressed as a singular H_∞ control problem [6]. The choice is largely a numerical matter - see [7] for a discussion of the numerical problems.

Now introduce the augmented signals

$$w = \begin{pmatrix} f \\ \psi \end{pmatrix}, \quad u = v, \quad z = \begin{pmatrix} d \\ \delta \end{pmatrix},, \quad y = e \qquad (20)$$

where the dimension of φ equals the dimension of e and the dimension of δ equals the dimension of v. Also introduce the augmented matrices

$$B_1 = (B_f \quad 0), \qquad B_2 = B_v, \quad C_1 = \begin{pmatrix} C_d \\ 0 \end{pmatrix}$$
$$D_{12} = \begin{pmatrix} 0 \\ \varepsilon_1 I \end{pmatrix}, \quad C_2 = C_e, \quad D_{21} = (0 \quad \varepsilon_2 I) \qquad (21)$$

With these definitions, the system (19) is transformed into

$$\begin{array}{ccccccc} \dot{x} & = & Ax & + & B_1 w & + & B_2 u \\ z & = & C_1 x & & & + & D_{12} u \\ y & = & C_2 x & + & D_{21} w \end{array} \qquad (22)$$

The two parameters $\varepsilon_1 > 0$ and $\varepsilon_2 > 0$ that are implicit in the direct feedthrough terms have the following interpretations. Firstly, ε_1 is a penalty on the control signal. Choosing ε_1 large will give relatively small control signals, whereas small values of ε_1 usually will give rather large controller gains. In a dual fashion, ε_2 is a measure of the allowable confidence in the measurements. In particular, selecting ε_2 large means that the measurements from an abstract design point of view are considered to be very noisy. Hence, only relatively small observer gains can be applied. Conversely, if ε_2 is chosen to be small, the quality of an observer estimating the states is not strongly restricted by noise, so typically the observer gains will be rather large.

It is easy to see that the closed loop transfer function from f to d in (19) has an H_∞ norm which is less than or equal to the H_∞ norm of the closed loop transfer function from w to z for system (22). Also as $\varepsilon_i \to 0$, $i = 1, 2$, the latter H_∞ norm tends to the former for the central controller. Hence (excluding detailed discussion for brevity) designing a controller for the system (22) will yield a controller that gives 'high performance' when applied to (19).

The actual selection of ε_1 and ε_2 is an iterative procedure. Intuitively, ε_1 relates to the feedback problem, whereas ε_2 relates to the estimation problem. Although the separation property of H_∞ theory is much more complicated than the similar property of H_2, in actual practice the selection of the two parameters can be done quite independently.

Hence, reasonable values of ε_1 and ε_2 can be obtained by two (convex) line searches. First, ε_1 is found, for example, by a bisection procedure to yield a value of the closed loop H_∞ norm which is sufficiently small, whilst keeping the controller gains reasonably bounded. This procedure is then repeated for ε_2.

A sample design (for the plant data and details of the disturbance force see [4]) is shown in Figure 2 (for a more detailed analysis see [8]) and shows that almost all the resonance peaks are significantly reduced - for the first modes this is up to 60 dB (Note the wide range logarithmic scale). In fact, as predicted, all resonance peaks above the average performance at low frequencies are drastically reduced. However (and surprisingly) even most of the peaks below DC-performance are reduced significantly as well. This is not a behavior that is inherent of H_∞ controllers. Actually, sometimes the 'flattening' property of H_∞ control can make the closed loop behavior for some frequency ranges worse than in open loop.

Fortunately, though, for the actual case, the computed central H_∞ controller achieves closed loop disturbance attenuation in all relevant frequency regions, in spite of the fact that a completely unweighted design was made. Hence, there is no need to introduce narrow band-pass dynamical weights for the optimization problem, could cause numerical and/or robustness problems.

Finally, it is instructive to consider the numerics of the problem. In particular, actual design reported here was undertaken for a LRR model with six modes in each direction, which means that the resulting standard problem was of order $2 \times 6^2 = 72$. Usually, this is not easily handled by the rather sensitive commercial software for H_∞ design. In the case discussed here, however, scaling the signals appropriately was all that was required for a successful optimization. In the guidelines for the use of H_∞ software it is sometimes recommended to use balanced realizations. With some effort it was possible to produce both a 72nd order balanced model as well as a reasonable 65th order reduced model for this case. It was not, however, possible to get the commercial software to work for the balanced models, which is probably due to the fact that the 'nice' second order block model structure was lost in the balancing process.

4 Conclusions

In this paper, H_∞ control design has been successfully applied the design of an active vibration damping system for a model of a spacecraft structure. The design was
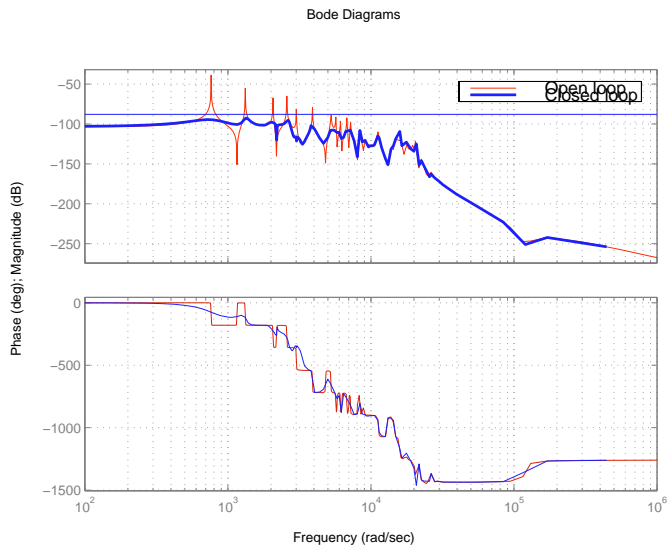
Figure 2: Open and closed loop transfer functions

based on a mechanical model obtained by the Lagrange-Rayleigh-Ritz approach. Although the model was of quite large order compared to most models used for control design, the model order was orders of magnitude smaller than that of a finite element model, which is not useful for controller design purposes.

H_∞ control design was an obvious choice, since the mechanical model already was in a four-block formulation; since the control objectives had natural frequency domain formulations; and since these objectives basically was a Bode-plot flatness condition.

The actual H_∞ design was based on a cheap control approach. It behaved exactly as predicted, except that (i) disturbance attenuations were almost better than hoped for, and (ii) high frequency behavior could be handled without introduction of weightings.

The design example given was based on a single input/single output control configuration. Some computational experiments were done also for the multivariable case, for which both the modeling and the control design technique applies equally well. It was anticipated that several actuator/sensor patches would improve performance significantly. However, the actual improvement turned out to be rather marginal. Therefore, the real benefit for using several patches seems to be in terms of control authority. For example, in an implementation it might be useful to have some physically small pairs of patches to handle high frequency behavior, and at the same time have pairs of patches of large physical dimensions to give control authority at low frequencies. A possible controller architecture would be parallel controllers, separated in frequency. Such controllers could easily be computed by adding two (first order) weights to the H_∞ standard problem formulation.

Currently in depth analysis of the design methodology given in this paper is being undertaken together with extensions to more complex geometries and/or loading patterns. Output from this research will be reported in due course.

References

[1] Stark H. R., and Stravrinidis C., "ESA Microgravity and Microdynamics Activities - An Overview", Acta Astronautica, **34**: 205-221, (1994).

[2] Zienkiewicz O. C., "The Finite Element Method", Mc-Graw Hill, London, (1977).

[3] Aglietti G. S., "Active Control of Microvibrations for Equipment Loaded Panels", PhD Thesis, University of Southampton, U.K. (1999).

[4] Aglietti G. S., Gabriel S. B., Langley R. S., and Rogers E., "A modeling technique for active control design studies with application to spacecraft microvibrations", Journal of the Acoustical Society of America, **102(4)**: 2158-2167, (1997).

[5] K. Zhou, J. C. Doyle and K. Glover. Robust and Optimal Control, New Jersey, Prentice-Hall, (1996).

[6] Stoorvogel A., "The H_∞ Control Problem: A State Space Approach", New Jersey, Prentice-Hall, (1992).

[7] Niemann H. H., and Stoustrup J., "Regular vs Singular Methods in Cheap H_∞ Control: A Numerical Study". In Proceedings of The European Control Conference, **2**: 733-738, (1993).

[8] Aglietti G. S., Stoustrup J., Rogers E., Langley R. S., and Gabriel S. B., "Robust control of microvibrations on mass loaded panels", Research Report, Dept Electronics and Computer Science, University of Southampton, UK (1999). (Also to be submitted to IEEE Transactions on Control Systems Technology.)